EPMA monazite geochronological constraints on the timing of ultra-high temperature reworking in the western Gawler Craton

Rian Dutch and Martin Hand

Report Book 2009/2

Government of South Australia
Primary Industries and Resources SA

202649

EPMA monazite geochronological constraints on the timing of ultra-high temperature reworking in the western Gawler Craton

Rian Dutch[1] and Martin Hand[2]

[1] Geological Survey Branch, Primary Industries and Resources South Australia

[2] Continental Evolution Research Group, School of Earth and Environmental Sciences, University of Adelaide

January 2009

Report Book 2009/2

Government of South Australia
Primary Industries and Resources SA

Division of Minerals and Energy Resources
Primary Industries and Resources South Australia
7th floor, 101 Grenfell Street, Adelaide
GPO Box 1671, Adelaide SA 5001

Phone	National	(08) 8463 3204
	International	+61 8 8463 3204
Fax	National	(08) 8463 3229
	International	+61 8 8463 3229
Email	pirsa.minerals@saugov.sa.gov.au	
Website	www.minerals.pir.sa.gov.au	

Preferred way to cite this publication
Dutch, R. and Hand, M., 2009. EPMA monazite geochronological constraints on the timing of ultra-high temperature reworking in the western Gawler Craton. *South Australia. Department of Primary Industries and Resources. Report Book,* 2009/2.

CONTENTS

FIGURES

EPMA monazite geochronological constraints on the timing of ultra-high temperature reworking in the western Gawler Craton

Rian Dutch and Martin Hand

ABSTRACT

New electron microprobe monazite geochronological constraints on the timing of granulite-facies metamorphism from the western Gawler Craton are presented. Monazite geochronology from the Ooldea DDH1 drill hole constrains the timing of granulite-facies metamorphism to *c.* 1700 Ma. The presence of two texturally distinct metamorphic assemblages in the Ooldea DDH2 drill hole suggests that the Moondrah Gneiss in this region underwent an early high-temperature low-pressure granulite-facies metamorphic event followed by ultra-high temperature high-pressure reworking associated with the development of the overprinting high-strain fabric. Monazite age data from the Ooldea DDH2 constrains the timing of the early metamorphic assemblage in Ooldea DDH2 to be *c.* 1690–1700 Ma in age, analogous to the *c.* 1700 Ma high-temperature low-pressure metamorphism recorded in Ooldea DDH1 and contemporaneous with the craton wide 1730–1690 Ma Kimban Orogeny. The later ultra-high temperature reworking event, termed the Ooldean Event, occurred at *c.* 1660 Ma.

INTRODUCTION

Despite the significant contribution of a number of recent studies (e.g. Howard et al., 2008; Payne, 2008; Payne et al., 2006; Payne et al., 2008; Swain et al., 2005b; Teasdale, 1997; Thomas et al., 2008), the geological evolution of the western Gawler Craton (Fig. 1, 2) remains enigmatic. This is primarily due to a lack of outcrop, meaning most geological interpretations are based on drill core and remote sensing techniques that don't necessarily allow for a rigorous interpretation of the geological history and development of the region. Despite the lack of a coherent geological framework, the western Gawler Craton is considered to be highly attractive to explorers, including existing heavy mineral deposits (e.g. Hou and Warland, 2005), and the potential for sedimentary uranium in the cover sequences and base metal (e.g. Ni) and gold mineralisation in the basement units.

Due to the absence of outcrop, the lithologies of the north-western Gawler Craton are known only from drill core. The Ooldea DDH1 stratigraphic hole (Figs 1, 2: Meyer, 1979) was drilled in 1976 by the Department of Mines and Energy South Australia (MESA) and intersected metasedimentary crystalline basement at *c.* 285 m. Following the discovery of potentially ultra-high temperature (UHT) sapphirine-bearing metasedimentary granulites (Purvis, 1981) in the region around the Ooldea siding, MESA drilled the stratigraphic Ooldea DDH2 diamond drill hole (Figs 1, 2: Daly, 1987). This hole intersected 63 m of layered high-grade quartz – feldspar – biotite – magnetite – cordierite – sillimanite – garnet bearing metasedimentary units, termed the Moondrah Gneiss (Daly et al., 1998). The Moondrah Gneiss is interpreted to comprise much of the western Gawler Craton north of the Karari Fault Zone (Figs 1, 2).

In this paper we present new electron microprobe (EPMA) monazite geochronological constraints on the timing of granulite-facies metamorphism in the Moondrah Gneiss. Monazite geochronology from Ooldea DDH1 constrains the timing of granulite-facies metamorphism to *c.* 1700 Ma, contemporaneous with the craton wide 1730–1690 Ma Kimban Orogeny (Dutch et al., 2008; Hand et al., 2007; Payne et al., 2008). The new age data from the Ooldea DDH2 drill hole constrains the timing of anhydrous UHT mylonitic reworking in the Moondrah Gneiss to *c.* 1660 Ma. This is in agreement with SHRIMP zircon U-Pb data presented by Fanning et al. (2007). However, this age is at odds with LA-ICP-MS age data from the same drill hole, which gave ages of *c.* 1690 Ma (Payne et al., 2008).

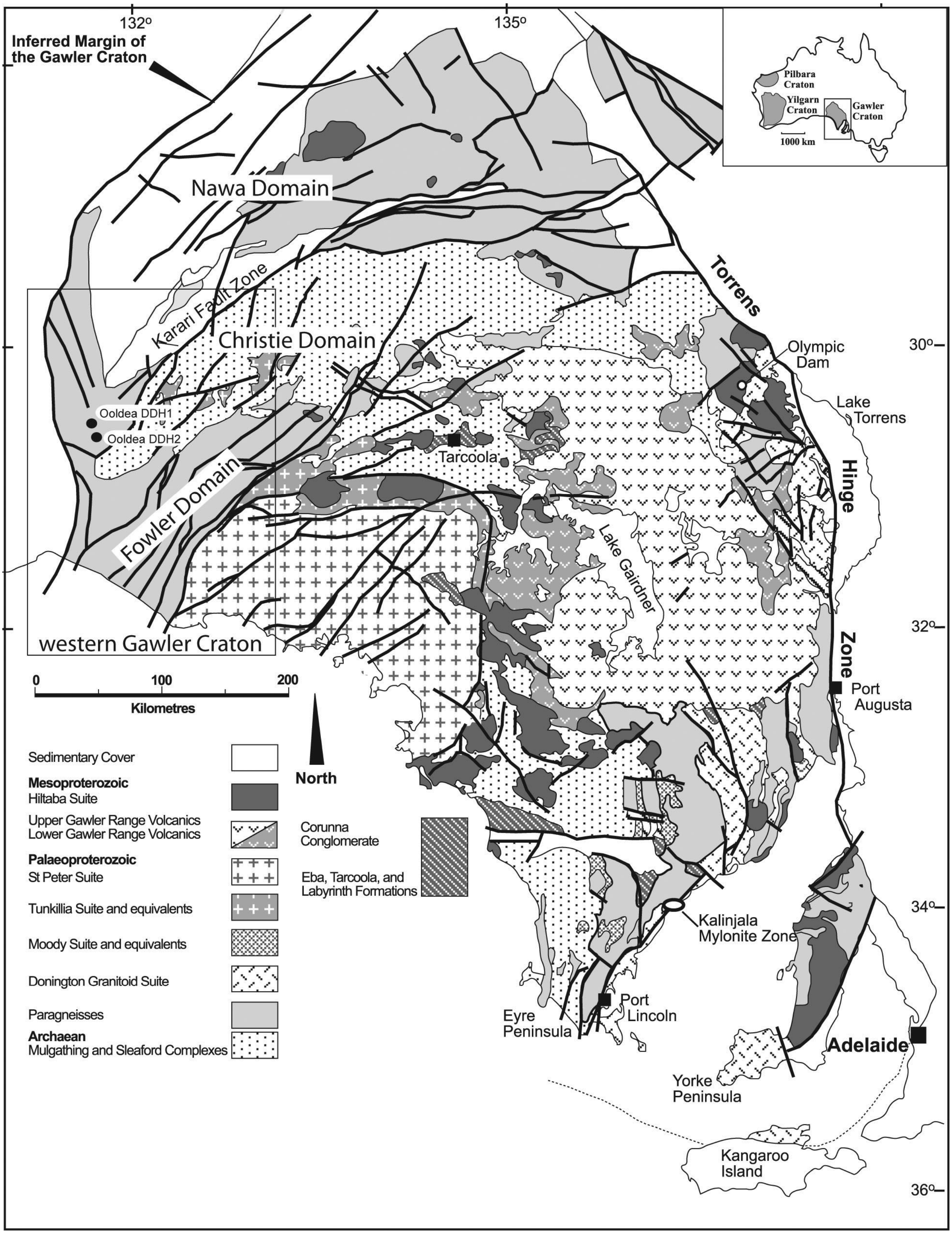

Figure 1. Simplified interpreted geology of the Gawler Craton (modified from Daly et al., 1998; Ferris et al., 2002). The box outlined the western Gawler Craton region containing the Ooldea 1 and Ooldea 2 drill hole locations.

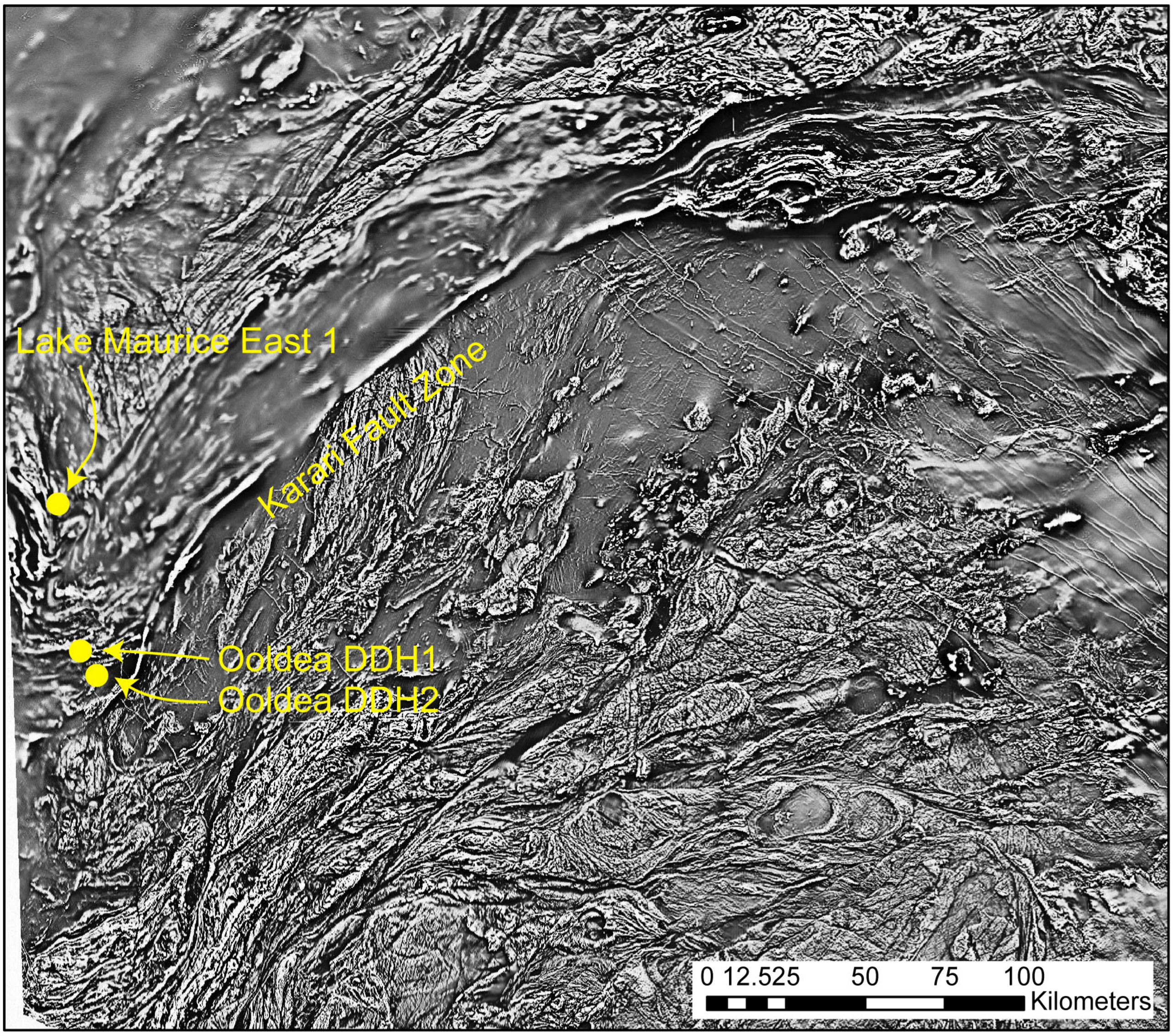

Figure 2. Regional 1st vertical derivative TMI image of the western Gawler Craton

GEOLOGICAL FRAMEWORK

REGIONAL GEOLOGY

The western Gawler Craton comprises all or part of the Nawa, Christie and Fowler Domains (Fig. 1: Daly et al., 1998; Ferris et al., 2002; Hand et al., 2007), which have been delineated largely based on geophysical character (Fig. 2), as the majority or the region is under Neoproterozoic and younger cover. The oldest known units are found in the Christie Domain, which comprises the Mulgathing Complex, and consists of interlayered metasedimentary, felsic and mafic orthogneiss, calc-silicates and metamorphosed banded iron formation (Daly et al., 1998; Hand et al., 2007; Swain et al., 2005a). These rocks were deformed and metamorphosed during the Sleafordian Orogeny between *c.* 2500-2420 Ma (McFarlane, 2006; Tomkins et al., 2004).

The Fowler Domain (Fig. 1) consists of a number of lithologies including mafic and ultra-mafic units, intermediate-felsic igneous and metasedimentary rocks (Daly et al., 1998; Teasdale, 1997; Thomas et al., 2008), including the 1690–1670 Ma Tunkillia Suite (Ferris and Schwartz, 2004; Payne, 2008; Teasdale, 1997). This region has been dissected by a number of regional scale shear zones (Fig. 2) which have been reactivated a number of times between 1700–1450 Ma (Fraser and Lyons, 2006; Swain et al., 2005b). Detrital zircon and monazite geochronology indicate the Fowler Domain sediments were deposited between *c.* 1770 Ma and 1730 Ma (Howard et al., 2008) and deformed and metamorphosed, together with the older Mulgathing Complex, at up to granulite-facies conditions during the Kimban Orogeny between *c.* 1730–1690 Ma (Howard et al., 2008; Teasdale, 1997).

Little is known about the western Nawa Domain. Two drill holes (Ooldea DDH1 and DDH2: Fig. 1) have intersected the Moondrah Gneiss, which is interpreted from geophysical evidence (Fig. 2) to dominate the lithology of the Nawa Domain (Teasdale, 1997). Teasdale (1997) described the geophysical character of the southern Nawa Domain as displaying a series of narrow (0.1–1km), parallel, linear, high magnetic intensity anomalies which form an arcuate, roughly northwest-trending belt of high average magnetic intensity. Weakly magnetised crust southwest of this belt exhibits weak linear trends which parallel the strongly magnetised linear anomalies. The parallel, strongly and weakly magnetised belts combine to define a *c.* 50 km wide, *c.* 120 km long, northwest trending mobile belt which transects the southern Nawa Domain. This belt is truncated to the east by the Karari Fault Zone, and to the west by a northeast-trending shear zone which juxtaposes it with the Murnaroo Platform (Fig. 2). Importantly, the Moondrah gneiss belt is paralleled by a coincident gravimetric high. The northwesterly trend of this mobile belt contrasts markedly with the dominantly northeasterly structural grain of the rest of the Nawa Domain. The linear magnetic highs which dominate the southern Nawa Domain are clearly caused by strongly magnetised, iron-rich gneiss (the Moondrah Gneiss) intersected in several drill holes, notably Ooldea DDH2.

In Ooldea DDH2, the dominant fabric is mylonitic and subvertical with a well-developed down dip mineral lineation associated with north-side up shear sense. This belt of reworking may extend as far north as Lake Maurice East (Fig. 2) which contains *c.* 1710 Ma granulite-facies assemblages that have undergone high-temperature mylonitic reworking (Payne et al., 2008). A provenance study by Payne et al. (2006) using detrital zircons from Ooldea DDH2 suggests the metasedimentary Moondrah Gneiss was deposited between 1740–1720 Ma.

EXISTING GEOCHRONOLOGICAL CONSTRAINTS ON THE MOONDRAH GNEISS

There have been a number of studies that have focused on the timing of metamorphism in the Moondrah Gneiss. Rb-Sr isotope data indicates that the Ooldea DDH2 drill core has a minimum metamorphic age of ~1700 Ma (Parker, 1993). Teasdale (1997) obtained a Pb-Pb evaporation age of 1690±9 Ma for interpreted metamorphic zircons from interval 153–154 in Ooldea DDH2. Fanning et al. (2007) presented U-Pb SHRIMP zircon data from a quartz – K-feldspar – plagioclase dominated lithology with minor garnet – orthopyroxene – sillimanite – spinel – magnetite from the 153.75–154 m interval. The zircons are interpreted to be metamorphic based on habit and Th/U ratio. Twenty analyses from twenty zircons produced a weighted mean age of 1659±6 Ma. Two older concordant analyses of *c.* 1700 Ma were excluded. Payne et al. (2008) analysed seven monazite grains from the interval 143–143.3 m via LA-ICP-MS in order to constrain the timing of high-grade metamorphism in the Moondrah Gneiss. They determined an age of 1691±10 Ma for the timing of metamorphic monazite growth, excluding one analysis which gave a Pb/Pb age of 1651±19 Ma.

Swain et al. (2005b) obtained EPMA monazite data from Ooldea DDH1 (288.7 m) and inferred an age of 1640±12 Ma for the granulite-facies metamorphism. However, due to methodological issues, the apparent age should be regarded as reconnaissance only.

PETROGRAPHY AND METAMORPHIC CONDITIONS OF THE MOONDRAH GNEISS

A thorough description of the petrography and interpreted metamorphism recorded in the Moondrah Gneiss from the Ooldea DDH2 drill hole is presented in Daly (1987) and Teasdale (1997), and the following is based largely on this work.

The Moondrah Gneiss in the Ooldea DDH2 drill hole consists of layered, magnetite-bearing, coarse grained granoblastic gneisses and includes Fe rich aluminous pelitic granulites. The metasedimentary units of the Moondrah Gneiss record a complex metamorphic history, with an early coarse-grained assemblage which underwent reworking to form a fine-grained high-strain assemblage.

The early coarse-grained assemblage is defined by cordierite – spinel – perthite – plagioclase – orthopyroxene – magnetite – quartz (Fig. 3a). Intergrowths of secondary orthopyroxene – sapphirine – K-feldspar – plagioclase – quartz (Fig. 3a) are interpreted to represent the former presence of osumalite as part of the early mineral assemblage. This assemblage is indicative of high-temperature low-pressure (HTLP) granulite-facies metamorphic conditions (e.g. Carrington and Harley, 1995; Kelsey, 2008; White et al., 2007).

The early high-grade mineral assemblage underwent structural reworking to produce an intense fine-grained gneissic layering which resulted in solid-state deformation of leucosomes associated with the early assemblage. This unit underwent a complex textural evolution which included; (a) the development of intergrown sillimanite and magnetite, (b) sapphirine, garnet and orthopyroxene coronas on magnetite, (c) corundum intergrowths with magnetite and quartz and (d) garnet – magnetite symplectites (Fig. 3b). This reworking also saw the break down of early cordierite to fine-grained symplectites of orthopyroxene – sillimanite – quartz (Fig. 2a), interpreted osumilite to fine-grained mosaics of orthopyroxene – sapphirine – K-feldspar – plagioclase – quartz (Fig. 3a) and the break down of early orthopyroxene to symplectites of sapphirine – cordierite. This reworking event was also marked by the recrystalisation of quartz and feldspar into the high-strain fabric and the development of quartz-ribbons.

Teasdale (1997) inferred peak pressure-temperature conditions in excess of 950°C and 9 kbar from thermobarometric constraints and the presence of stable coexisting sapphirine – quartz (Fig. 3c), spinel – quartz and mesoperthite – antiperthite assemblages and the high Al content (up to 10 wt%) in orthopyroxene, which are all indicative of UHT metamorphism (Harley, 2008; Kelsey, 2008).

The Moondrah Gneiss from the Ooldea DDH1 drill hole contains a simpler petrographic record (Meyer, 1979; Swain et al., 2005b). This unit consists of a garnet – sillimanite – cordierite – magnetite – biotite – perthite-bearing assemblage (Figs 3d, e, f). This assemblage is typical of HTLP granulite-facies conditions (e.g. White et al., 2007). Subsequent retrogression has resulted in most of the cordierite being replaced by clay minerals and significant replacement of feldspars by sericite.

ANALYTICAL METHODS

In order to constrain the timing of peak metamorphic conditions in Ooldea DDH1, one sample containing the peak assemblage was selected for monazite EPMA geochronology. Similarly, to constrain UHT reworking in the Moondrah Gneiss from Ooldea DDH2, samples from four different depths were selected for monazite EPMA geochronology. Each interval was selected because it contained a fine-grained high-strain to mylonitic fabric and sapphrine-bearing mineral assemblages. Samples 43, 73, 94 and 136 come from depths 43 m, 73 m, 94 m and 136 m respectively. All selected monazites were located within the high-strain fabric at grain boundaries. Prior to analysis, monazites were BSE imaged using a Phillips XL20 SEM with a 15 kV accelerating voltage and a 20 nA beam current, at Adelaide Microscopy in the University of Adelaide (Fig. 4).

EPMA monazite chemical dating (e.g. Montel et al., 1996; Williams and Jercinovic, 2002), uses an electron microprobe to measure the total amounts of U, Th and Pb in monazite. Monazite is typically very rich in the radioactive elements U and Th, and therefore radiogenic Pb accumulates at a rate such that measurable quantities (>300 ppm) of Pb are reached in about 100 Ma (Montel et al., 2000). Previous studies (e.g. Parrish, 1990) have demonstrated that monazite contains negligible common Pb compared with the radiogenically produced component; therefore it can be reasonably assumed that essentially all measured Pb in monazite is the result of the radiogenic breakdown of Th and U.

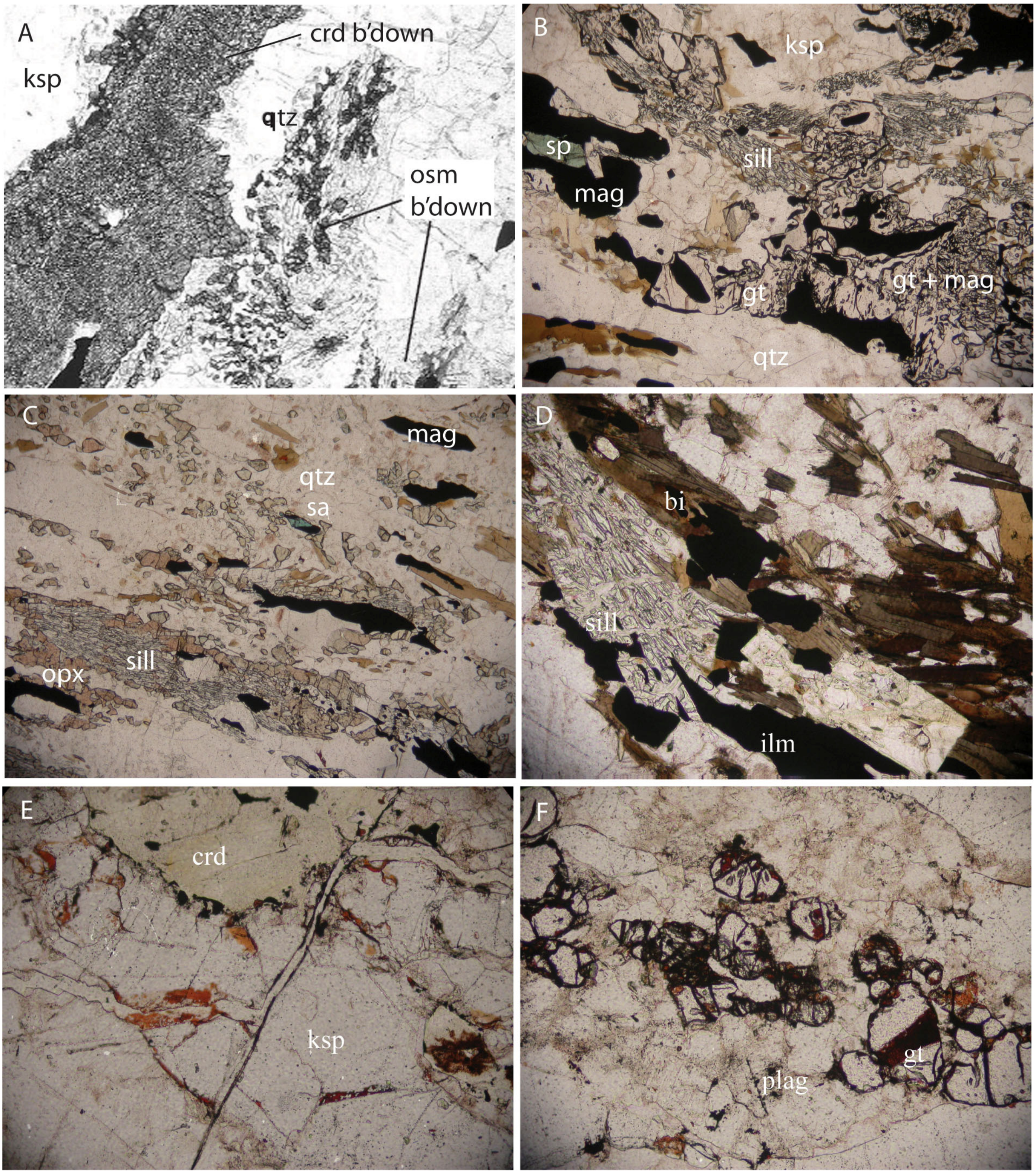

Figure 3. Photomicrographs of the Moondrah Gneiss assemblages. (A) Primary metamorphic assemblage from Ooldea 2 (from Teasdale 1997). (B & C) Fine grained UHT reworking assemblages from Ooldea 2. (D, E & F) Coarse pelitic HTLP assemblage from Ooldea 1.

Analyses of monazite were conducted using a Cameca SX51 Electron Microprobe, at Adelaide Microscopy in the University of Adelaide. A thorough description of the method used is presented in Dutch (2009). Analyses were run at an accelerating voltage of 20 kV and a 100 nA beam current. Th, U, Pb and Ce were analysed concurrently with PET crystals using the Mα line for Th, Mβ lines for Pb and U and Lα line for Ce. The standards used were huttonite (Th), UO_2, synthetic Pb glass (K227) and single element REE glasses. The full range of elements which are typically partitioned into monazite were analysed. Offline corrections were made to account for an overlap of the second order Ce Lα escape peak with the required Pb Mβ peak (Pyle et al., 2005), and overlaps of the Th Mγ peak on U Mβ line and U Mz_2 on Pb Mβ. The ages for each spot were then determined using the Th-U-Pb concentrations and the statistical methods outlined in Montel et al. (1996). Probe element calibration was tested against the standards, with analysed concentrations for U, Th, Pb and Ce being ±0.5% of the standard composition. All other elements were within ±1% of the standard composition. Probe performance was monitored by comparison with a 518 Ma monazite standard with known U-Th-Pb concentrations. Reproducibility of the standard during the course of the analytical sessions (n = 80) was 523±8 Ma (2σ) (MSWD 1.0). Statistical analysis of the geochronological data was performed using the Excel add-in ISOPLOT (Ludwig, 2003).

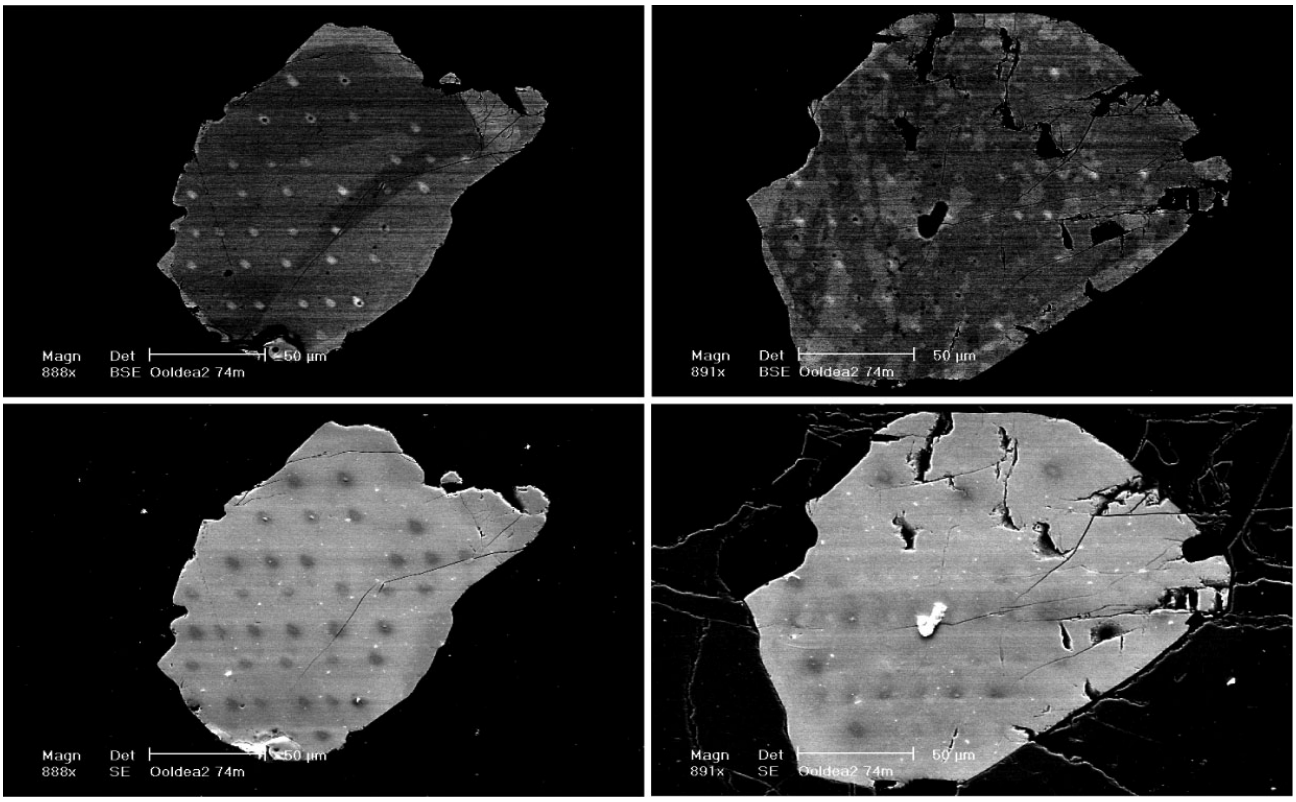

Figure 4. Representative BSE (top) and SE (bottom) images of monazites from Ooldea 2

EPMA MONAZITE RESULTS

Analysed monazites were between 20–100 µm in diameter, sub- to anhedral in habit and displayed either no zoning or complex zoning in BSE images with up to two different domains (Fig. 4). However, no correlation was discerned between age and chemical domain.

Six monazite grains from the Ooldea DDH1 sample were analysed and produced a weighted mean age of 1700±11 Ma (n = 50, MSWD 1.2). A relative probability plot of this data (Fig. 5) shows a unimodal age population.

From Ooldea DDH2, three monazites from Sample 43 were analysed and produced a weighted average age of 1666±12 Ma (n = 83, MSWD 1.17). However, a relative probability plot of this data (Fig. 5) suggests there may be two significant age peaks. A statistical unmixing of this data (Sambridge and Compston, 1994) produces two weighted mean ages of 1649±16 Ma and 1727±27 Ma. However, no correlation between age and chemical domain or textural setting was observed.

Five monazite grains from Sample 73 were analysed and produced a weighted average age of 1656±16 Ma (n = 72, MSWD 1.8). The relative probability plot (Fig. 5) suggests there may be distinct age peaks at *c.* 1700 Ma and *c.* 1640 Ma but unlike sample 43 the ages cannot be separated statistically. A few analyses with apparent ages >1800 Ma may reflect remnant detrital monazite.

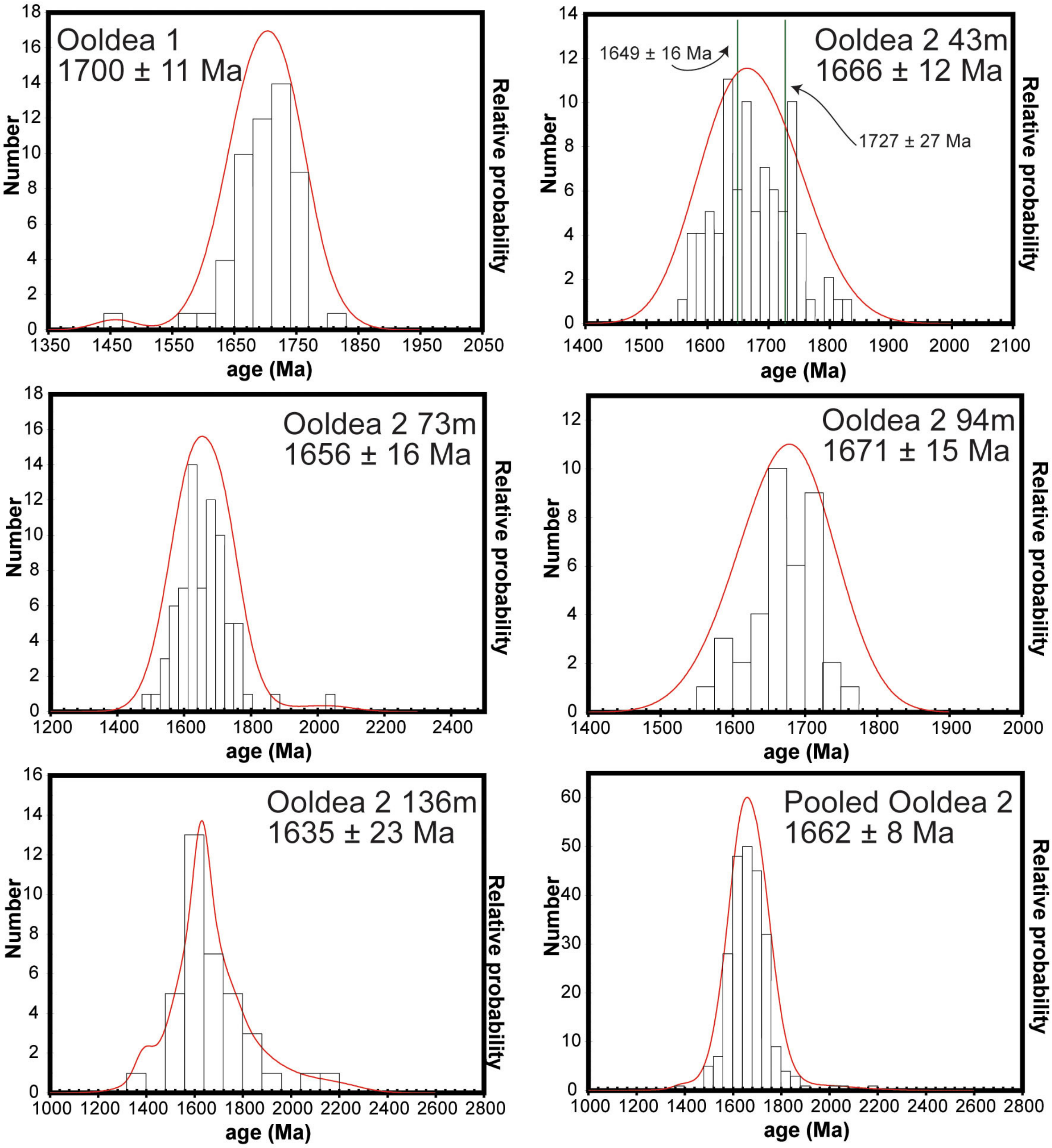

Figure 5. Relative probability plots for EPMA monazite data from Ooldea 1 and Ooldea 2 monazites

Five monazite grains from Sample 94 produced a weighted mean average age of 1671±15 Ma (n = 38, MSWD 0.97). As with the previous samples there is a suggestion of distinct peaks at *c.* 1650 Ma and *c.* 1700 Ma (Fig. 5). Based on age alone, these peaks can not be statistically separated.

Five monazites from Sample 136 produced a weighted average age of 1635±23 Ma (n = 34, MSWD 1.5). The relative probability plot (Fig. 5) displays a unimodal peak and *c.* 1640 Ma with a couple of analyses >1800 Ma which may reflect remnant detrital monazite. Combining all the data from each sample produces a single unimodal peak (Fig. 5) with a weighted average age of 1662±8 Ma (n = 227, MSWD 1.4).

DISCUSSION

The EPMA monazite results presented here suggest two metamorphic events are recorded in the Moondrah Gneiss in the western Gawler Craton. The age of 1700±11 Ma from monazites within a HTLP granulite-facies metapelite from Ooldea DDH1 suggests the Moondrah Gneiss was metamorphosed and deformed during the craton wide 1730–1690 Ma Kimban Orogeny (Dutch et al., 2008; Hand et al., 2007; Payne et al., 2008). This is consistent with the LA-ICP-MS monazite data of Payne et al. (2008) which suggest that metamorphic monazite grew in the Moondrah Gneiss of Ooldea DDH2 at 1691±10 Ma. The EPMA monazite geochronology presented here from the fine-grained UHT reworked assemblage from Ooldea DDH2 suggests that the reworking occurred at *c.* 1660 Ma. This is consistent with the SHRIMP U-Pb age data from metamorphic zircons from the Ooldea DDH2 core which give a metamorphic age of 1659±7 Ma (Fanning et al., 2007). However there is a suggestion of two age populations in the data of Fanning et al., (2007) with unmixing (Sambridge and Compston, 1994) of the spot ages yielding 1649±7 Ma (77% of analyses) and 1693±9 Ma (23% of analyses). The older of these ages is identical to the LA-ICP-MS monazite age obtained by Payne et al (2008) and the Pb-Pb zircon evaporation age of 1690±9 Ma of Teasdale (1997), and is similar to the suggestion of a population of *c.* 1700 Ma monazite in three of the four samples analysed in this study from Ooldea DDH2. The younger of the unmixing ages derived from Fanning et al (2007) is within error of the overall population average of the EPMA monazite data obtained in this study, and also the younger of the apparent bi-modal age groups.

The presence of two texturally distinct metamorphic assemblages in the Ooldea DDH2 core suggests that the Moondrah Gneiss in this region underwent an early HTLP granulite-facies metamorphic event followed by UHT high-pressure reworking associated with the development of the overprinting high-strain fabric. We interpret the early metamorphic assemblage in Ooldea DDH2 to be *c.* 1690–1700 Ma in age and analogous to the *c.* 1700 Ma HTLP metamorphism recorded in Ooldea DDH1. This metamorphism was part of craton wide tectonism associated with the Kimban Orogeny (e.g. Dutch et al., 2008; Hand et al., 2007; Payne et al., 2008). The later UHT reworking event, termed the Ooldean Event by Hand et al. (2007), is at present spatially unconstrained. However as noted above, regional magnetic data shows a distinctive magnetic domain in the western Gawler Craton that incorporates Ooldea DDH2 and also the reworked granulites intersected in Lake Maurice East (Fig. 2), suggesting the region of UHT reworking may be significant in extent. This would be consistent with the intensity of the metamorphism, which requires large-scale thermal perturbation of the crust. The inferred age of the UHT reworking in the Moondrah Gneiss is also identical to the depositional age of the volcanic associated Tarcoola Formation (Budd, 2006; Daly et al., 1998) suggesting a widespread region of thermally perturbed crust at *c.* 1650 Ma.

The monazite age data obtained from Ooldea DDH2 raises questions about the stability of monazite in high-grade metamorphic rocks. Payne et al (2008) obtained an age of 1691±10 Ma, whereas the bulk of the monazite ages obtained in this study are around 1660 Ma, and similar to the bulk of the zircon ages obtained by Fanning et al., (2007).

Monazite is generally suspected to be more susceptible to resetting than zircon (Kelsey et al., 2008) due to its comparative chemical reactivity (e.g. Bea and Montero, 1999; Spear and Pyle, 2002). However, in the case of Ooldea DDH2, monazite analysed by Payne et al. (2008) still retains Kimban ages-despite being overprinted by UHT (>900) conditions. For the monazite grain sizes analysed by Payne et al (2008) 150–300 micron, very high Pb closure temperatures are predicted using experimental diffusion data ~1000–1100°C (Cherniak et al., 2004). The estimated closure temperatures imply that, providing the crystal lattice of these minerals remains intact, even UHT conditions will not reset the monazite U-Pb isotopic systems via volume diffusion. In general the monazite grains analysed in this study are smaller than those targeted by Payne et al (2008). We suggest that the relatively anhydrous and non-migmatitic conditions associated with the reworking recorded in Ooldea DDH2 favoured the preservation of the Kimban-aged, comparatively coarse-grained monazite grains whereas the smaller grains targeted in this study either underwent volume diffusion during reworking or recrystallised with the fine-grained fabric. However the suggestion of a *c.* 1700 Ma monazite population in 3 of the samples anaylsed in this study suggest that even in the grains that we targeted significant volumes of the monazite essentially retain their original growth age despite later UHT conditions.

REFERENCES

Bea, F. and Montero, P., 1999. Behavior of accessory phases and redistribution of Zr, REE, Y, Th, and U during metamorphism and partial melting of metapelites in the lower crust: An example from the Kinzigite Formation of Ivrea-Verbano, NW Italy. Geochimica et Cosmochimica Acta, 63: 1133-1153.

Budd, A., 2006. The Tarcoola Goldfield of the central Gawler gold province, and the Hiltaba Association Granites, Gawler Craton, South Australia. PhD Thesis, Australian National University, Canberra, 365 pp.

Carrington, D.P. and Harley, S.L., 1995. The Stability of Osumilite in Metapelitic Granulites. Journal of Metamorphic Geology, 13(5): 613-625.

Cherniak, D.J., Watson, E.B., Grove, M. and Harrison, T.M., 2004. Pb diffusion in monazite: a combined RBS/SIMS study. Geochimica et Cosmochimica Acta, 68(4): 829-840.

Daly, S.J., 1987. Ooldea 2 - Well Completion Report. Mines and Energy, South Australia. Report Book, 87/48.

Daly, S.J., Fanning, C.M. and Fairclough, M.C., 1998. Tectonic evolution and exploration potential of the Gawler Craton, South Australia. AGSO Journal of Australian Geology and Geophysics, 17(3): 145-168.

Dutch, R., Hand, M. and Kinny, P., 2008. High-grade Palaeoproterozoic reworking in the southeastern Gawler Craton, South Australia. Australian Journal of Earth Sciences, 55: 1063-1081.

Dutch, R.A., 2009. Reworking the Gawler Craton: Metamorphic and geochronologic constraints on Palaeoproterozoic reactivation of the southern Gawler Craton. Ph.D Thesis, University of Adelaide, Adelaide, 233 pp.

Fanning, C.M., Reid, A.J. and Teale, G.S., 2007. A geochronological framework for the Gawler Craton, South Australia. South Australia Geological Survey, Bulletin, 55.

Ferris, G.M. and Schwartz, M.P., 2004. Definition of the Tunkillia Suite, western Gawler Craton. MESA Journal, 34: 32-41.

Ferris, G.M., Schwartz, M.P. and Heithersay, P., 2002. The geological framework, distribution and controls of Fe-oxide related alteration, and Cu-Au mineralisation in the Gawler Craton, South Australia: Part 1: Geological and tectonic framework. In: T.M. Porter (Editor), Hydrothermal Iron Oxide Copper-Gold and Related Deposits: A Global Perspective, Volume 2. PGC Publishing, Adelaide.

Fraser, G.L. and Lyons, P., 2006. Timing of Mesoproterozoic tectonic activity in the northwestern Gawler Craton constrained by Ar-40/Ar-39 geochronology. Precambrian Research, 151(3-4): 160-184.

Hand, M., Reid, A. and Jagodzinski, L., 2007. Tectonic framework and evolution of the Gawler craton, southern Australia. Economic Geology, 102(8): 1377-1395.

Harley, S.L., 2008. Refining the P-T records of UHT crustal metamorphism, pp. 125-154.

Hou, B. and Warland, I., 2005. Heavy mineral potential of Eucla Basin, SA - a world-class palaeo-beach placer province. MESA Journal, 37: 4-12.

Howard, K., Dutch, R., Hand, M., Barovich, K.M. and Reid, A., 2008. Unravelling the Fowler Domain: new geochronological data from the western Gawler Craton, South Australia. South Australia. Department of Primary Industries and Resources. Report Book, 2008/10.

Kelsey, D.E., 2008. On ultrahigh-temperature crustal metamorphism. Gondwana Research, 13(1): 1-29.

Kelsey, D.E., Clark, C. and Hand, M., 2008. Thermobarometric modelling of zircon and monazite growth in melt-bearing systems: examples using model metapelitic and metapsammitic granulites. Journal of Metamorphic Geology, 26: 199-212.

Ludwig, K.R., 2003. Users Manual for Isoplot/Ex, Version 3.00, A Geochronological Toolkit for Microsoft Excel. Berkeley Geochronology Centre, Berkeley, CA, 2003. Special Publication No.4.

McFarlane, C.R.M., 2006. Palaeoproterozoic evolution of the Challenger Au Deposit, South Australia, from monazite geochronology. Journal of Metamorphic Geology, 24(1): 75-87.

Meyer, G., 1979. Ooldea No. 1 and Reid Nos 1 and 1a well completion report. Department of Mines and Energy South Australia. Report Book, 79/83.

Montel, J.M., Foret, S., Veschambre, M., Nicollet, C. and Provost, A., 1996. Electron microprobe dating of monazite. Chemical Geology, 131: 37-53.

Montel, J.M., Kornprobst, J. and Vielzeuf, D., 2000. Preservation of old U-Th-Pb ages in shielded monazite; example from the Benmi Bousera Hercynian kinzigites (Morocco). Journal of Metamorphic Geology, 18(3): 335-342.

Parker, A.J., 1993. Palaeoproterozoic. In: J.F. Drexel, W.V. Preiss and A.J. Parker (Editors), The geology of South Australia; Volume 1, The Precambrian. Bulletin 54- Geological Survey of South Australia, pp. 50-105.

Parrish, R.R., 1990. U-Pb dating of monazite and its application to geological problems. Canadian Journal of Earth Sciences, 27(11): 1431-1450.

Payne, J.L., 2008. Palaeo- to Mesoproterozoic Evolution of the Gawler Craton, Australia: Geochronological, geochemical and isotopic constraints. Ph.D Thesis, University of Adelaide, Adelaide.

Payne, J.L., Barovich, K.M. and hand, M., 2006. Provenance of metasedimentary rocks in the northern Gawler Craton, Australia: Implications for Palaeoproterozoic reconstructions. Precambrian Research, 148(3-4): 275-291.

Payne, J.L., Hand, M., Barovich, K.M. and Wade, B.P., 2008. Temporal constraints on the timing of high-grade metamorphism in the northern Gawler Craton: implications for assembly of the Australian Proterozoic. Australian Journal of Earth Sciences, 55(5): 623-640.

Purvis, A.C., 1981. Pontifex & Associates: Mineralogical report No. 3343. In; Miller, G. Report on EL616. South Australian Department of Mines and Energy Open File Envelope 3855.

Pyle, J.M., Spear, F.S., Wark, D.A., Daniel, C.G. and Storm, L.C., 2005. Contributions to precission and accuracy of monazite microprobe ages. American Mineralogist, 90: 547-577.

Sambridge, M.S. and Compston, W., 1994. Mixture modelling of multi-component data sets with application to ion-probe zircon ages. Earth and Planetary Science Letters, 128: 373-390.

Spear, F.S. and Pyle, J.M., 2002. Apatite, monazite, and xenotime in metamorphic rocks. In: J. Kohn Matthew, J. Rakovan and M. Hughes John (Editors), Phosphates; geochemical, geobiological, and materials importance.

Swain, G. et al., 2005a. Provenance and tectonic development of the late Archaean Gawler Craton, Australia; U-Pb zircon, geochemical and Sm-Nd isotopic implications. Precambrian Research, 141(3-4): 106-136.

Swain, G.M., Hand, M., Teasdale, J., Rutherford, L. and Clark, C., 2005b. Age constraints on terrane-scale shear zones in the Gawler Craton, southern Australia. Precambrian Research, 139(3-4): 164-180.

Teasdale, J., 1997. Methods for understanding poorly exposed terrains: The interpretive geology and tectonothermal evolution of the western Gawler craton. Ph.D. Thesis, University of Adelaide, Adelaide, 182 pp.

Thomas, J.L., Direen, N.G. and Hand, M., 2008. Blind orogen: Integrated appraisal of multiple episodes of Mesoproterozoic deformation and reworking in the Fowler Domain, western Gawler Craton, Australia. Precambrian Research, 166(1-4): 263-282.

Tomkins, A.G., Dunlap, W.J. and Mavrogenes, J.A., 2004. Geochronological constraints on the polymetamorphic evolution of the granulite-hosted Challenger gold deposit: implications for assembly of the northwest Gawler Craton. Australian Journal of Earth Sciences, 51(1): 1-14.

White, R.W., Powell, R. and Holland, T.J.B., 2007. Progress relating to calculation of partial melting equilibria for metapelites. Journal of Metamorphic Geology, 25(5): 511-527.

Williams, M.L. and Jercinovic, M.J., 2002. Microprobe monazite geochronology; putting absolute time into microstructural analysis. Journal of Structural Geology, 24: 1013-1028.